JOURNAL OF VIROLOGY, Mar. 2004, p. 3089–3098 Vol. 78, No. 6
0022-538X/04/$08.00+0 DOI: 10.1128/JVI.78.6.3089–3098.2004


# Cholesterol Is Required for Endocytosis and Endosomal Escape of Adenovirus Type 2

Nicola Imelli,[1] Oliver Meier,[1] Karin Boucke,[1] Silvio Hemmi,[2] and Urs F. Greber[1]*

*Zoologisches Institut[1] and Institut für Molekularbiologie,[2] Universität Zürich, CH-8057 Zürich, Switzerland*

Received 19 September 2003/Accepted 20 November 2003

**The species C adenovirus type 2 (Ad2) and Ad5 bind the coxsackievirus B Ad receptor and αv integrin coreceptors and enter epithelial cells by clathrin-mediated endocytosis. This pathway is rapid and efficient. It leads to cell activation and the cholesterol-dependent formation of macropinosomes. Macropinosomes are triggered to release their contents when incoming Ad2 escapes from endosomes. Here, we show that cholesterol extraction of epithelial cells by methyl-β-cyclodextrin (mβCD) treatment reduced Ad5-mediated luciferase expression ~4-fold. The addition of cholesterol to normal cells increased gene expression in a dose-dependent manner up to threefold, but it did not restore gene expression in mβCD-treated cells. mβCD had no effect in the presence of excess cholesterol, indicating that the inhibition of gene expression was due specifically to cholesterol depletion. Cholesterol depletion inhibited rapid Ad2 endocytosis, endosomal escape, and nuclear targeting, consistent with the notion that clathrin-dependent endocytosis of Ad2 is cholesterol dependent. In cholesterol-reduced cells, Ad2 internalized at a low rate, suggestive of an alternative, clathrin-independent, low-capacity entry pathway. While exogenous cholesterol completely restored rapid Ad2 endocytosis, macropinocytosis, and macropinosome disruption, it did not, surprisingly, restore viral escape from endosomes. Our results indicate that macropinosome disruption and endosomal escape of Ad2 are independent events in cells depleted of and then refilled with cholesterol, suggesting that viral escape from endosomes requires lipid-controlled membrane homeostasis, trafficking, or signaling.**

The plasma membrane is a major barrier for invading agents. It is organized into microdomains coupling the entry of receptor-bound ligands to the internal organization of the cell. Viruses penetrate the plasma membrane by various mechanisms, including lipid fusion and membrane perforation, or they enter by receptor-mediated endocytosis, bypassing the cortical actin network (27, 36, 55, 60). Endocytosis is crucial for cell homeostasis, regulation of activation, and viral infection (for recent reviews, see references 9, 15, and 44). All types of endocytosis are harnessed by viruses (reviewed in references 40, 55, and 61). Clathrin-dependent endocytosis requires the large GTPase dynamin, a variety of additional factors, and sometimes also lipid rafts that are cholesterol dependent. It originates at specialized plasma membrane regions where cytosolic adaptor proteins bind the endocytic receptors and phosphoinositides, allowing the formation of clathrin coats (for a recent review, see reference 31). Clathrin-dependent endocytosis is used by a variety of enveloped viruses, such as Semliki Forest virus (24), Sindbis virus (12), vesicular stomatitis virus (71), Hantaan virus (29), and influenza virus (37), although for the last a clathrin-independent pathway has also been proposed (63). Clathrin-dependent endocytosis is apparently used by nonenveloped viruses, such as parvoviruses (4, 54), human rhinovirus type 2 (67), human papillomavirus types 16 and 58 (6), and human adenovirus type 2 (Ad2) and Ad5 (7, 16, 39, 42, 75, 76). With other viruses, the evidence for or against clathrin-dependent endocytosis is not so clear.

Caveolar uptake and lipid raft-dependent pathways invariably require cholesterol, and sometimes the coat protein caveolin 1, and dynamin, a large GTPase implicated in pinching off the emerging membrane buds (reviewed in reference 74). Caveolae are flask-shaped invaginations of the plasma membrane, important for cell signaling, cholesterol efflux, and the uptake of cholesterol esters. In normal tissue culture cells, caveolae do not pinch off, but simian virus 40, polyomavirus, echovirus 1, and certain filoviruses can induce the internalization of caveolae (reviewed in reference 55). Caveolin-independent uptake can be dynamin dependent, as in the case of the interleukin 2 receptor (33) or intercellular adhesion molecule 1 (43). Intercellular adhesion molecule 1 serves as a receptor of the major group of human rhinoviruses and coxsackievirus A21 (reviewed in references 5 and 27), implying that these agents can be taken up by uncoated membranes. In turn, caveolin-independent uptake can be independent of dynamin, e.g., the raft-dependent macropinocytosis (10, 23, 39) and a less well-characterized raft-independent endocytic pathway (30, 51). Interestingly, virus-like particles of human papillomavirus type 16 appear to enter Langerhans cells by a clathrin- and macropinocytosis-independent pathway but enter dendritic cells by a clathrin-dependent pathway, indicating cell-type-specific differences (14). Macropinocytosis in turn has a key role in the entry of *Chlamydia*, *Salmonella*, *Shigella*, and *Brucella* bacteria (49, 53, 77) and perhaps human immunodeficiency virus type 1 (34). It is induced by growth factor stimulation or downstream signaling molecules in epithelial cells, fibroblasts, neutrophils, macrophages, and dendritic cells and leads to the closure of lamellipodia at ruffling membranes, thus engulfing large areas of plasma membrane (25).

Given that viruses enter by various endocytic pathways, the question of how a particular pathway is selected arises. Besides

* Corresponding author. Mailing address: Zoologisches Institut der Universität Zürich, Winterthurerstrasse 190, CH-8057 Zürich, Switzerland. Phone: 41 1 635 4841. Fax: 41 1 635 6822. E-mail: ufgreber@zool.unizh.ch.

cell-type-specific aspects, crucial determinants are the cell surface receptors and coreceptors. Serotypes of the human Ad species A, C, D, E, and F bind the coxsackievirus B Ad receptor (CAR) (59), whereas serotypes of the two species B1 and B2 use the membrane cofactor CD46 as a receptor (17, 62; D. Sirena, B. Lilienfeld, M. Eisenhut, S. Kaelin, K. Boucke, R. R. Beerli, L. Vogt, C. Ruedl, M. F. Bachmann, U. F. Greber, and S. Hemmi, submitted for publication). While the internalization pathways of the species B Ads are unknown, the species C Ads are internalized into epithelial cells through clathrin-dependent endocytosis activated by αvβ3 or αvβ5 integrin coreceptors (for reviews, see references 40 and 48). Recent evidence suggests that CAR is associated with GM1 ganglioside-containing lipid raft microdomains that are disrupted by the cholesterol-binding reagent methyl-β-cyclodextrin (mβCD), thus inhibiting infection (3).

Here, we show that cholesterol is required for rapid Ad2 endocytosis, macropinocytosis, viral escape, and infection. In cholesterol-reduced cells, we find evidence of a slow Ad2 internalization pathway delivering low levels of virus to the cytosol. Surprisingly, cholesterol replacement did not restore infection and viral escape from endosomes, although it restored endocytosis, macropinocytosis, and macropinosomal disruption, implying that cholesterol-dependent membrane trafficking is directly or indirectly implicated in Ad2 escape from endosomes. These results raise the notion that the entry of both nonenveloped and enveloped viruses, as well as bacterial pathogens (8, 32, 56), can be dependent on cellular cholesterol.

## MATERIALS AND METHODS

**Cells, viruses, plasmids, and proteins.** HeLa cells (human cervical epitheloid carcinoma cells) were grown in Dulbecco's modified Eagle's medium (DMEM) (Gibco-BRL, Basel, Switzerland) containing 7% clone III serum or 7% fetal bovine serum (HyClone; Integra BioSciences AG, Zürich, Switzerland), 1% nonessential amino acids, and 1% glutamine (Gibco-BRL). Ad2 and [$^{35}$S]methionine-labeled Ad2 were purified and labeled with Texas Red (TR) as described previously (18, 21, 47). Cell binding of [$^{35}$S]methionine-labeled Ad2 (75,000 cpm per μl) was performed as described previously (39). *ts*1 Ad2 (a temperature-sensitive virus lacking functional p23 protease) (78) was produced as described previously (20). Ad5-Luc (with the E1A and E1B regions deleted and containing the firefly luciferase gene (*luc*) under the control of the major cytomegalovirus [CMV] promoter) was used as described previously (35). The pAd-CMV-*luc* plasmid was supplied by D. Sirena (University of Zürich). Ad2 fiber knob (0.4 mg/ml) and cyclic arginine-glycine-aspartate peptide (cRGD; 0.1 mM) were used as reported previously (70). The mouse monoclonal anti-CAR antibody E1-1 (13) and the function-blocking anti-αv integrin mouse monoclonal antibody 17E6 (41) were employed as described previously (45).

**Metabolic labeling.** HeLa cells grown in 35-mm-diameter dishes were incubated in methionine-free, serum-free medium (Gibco) at 37°C for 20 min and pulse-labeled with 5 μCi of Tran-[$^{35}$S]-Label (1,175 Ci/mmol; ICN Biochemicals) for 40 min, extensively washed with phosphate-buffered saline (PBS), and lysed in 1 ml of Ripa buffer (20 mM Tris-HCl, pH 7.4, 130 mM NaCl, 2 mM EDTA, 0.1% sodium dodecyl sulfate, 0.5% deoxycholate, 1% Triton X-100) containing protease inhibitors (1 mM phenylmethylsulfonyl fluoride and 1 μg each of chymostatin, leupeptin, aprotinin, and pepstatin/ml) at 4°C for 30 min as described previously (46). The lysate was precipitated with trichloroacetic acid (15% [wt/vol]) on ice for 30 min and centrifuged at 16,000 × *g* for 10 min at 4°C. The pellet was washed in ice-cold acetone, centrifuged, air dried, dissolved in 200 μl of 0.1 M Tris (pH 8.1) containing 1% sodium dodecyl sulfate, and analyzed in a liquid scintillation counter (Beckman) as described previously (73).

**Luciferase activity.** Ad5-Luc was titrated by plaque assays on 911 cells expressing E1 proteins (45). It was bound to HeLa cells in 24-well dishes in cold RPMI-bovine serum albumin (BSA) for 1 h and internalized in DMEM-BSA at 37°C for various times. The cells were washed with PBS and lysed in 400 μl of buffer mixture (Promega), and luciferase activity was quantitated as described previously (35). The results were normalized to the cell numbers for each condition as determined in parallel samples using crystal violet. The activity of CMV promoter-controlled luciferase DNA was determined upon electroporation of 5 μg of pAd-CMV-*luc* DNA per $10^6$ cholesterol-depleted or normal cells (Nucleofector; Amaxa GmbH, Cologne, Germany).

**Cholesterol depletion and replacement.** HeLa cells grown in 35-mm-diameter dishes to 80% confluency had their cholesterol reduced either with 4 μM lovastatin (LOV; Merck, Darmstadt, Germany) and 0.25 mM mevalonate (MEV; Sigma, Fluka, Switzerland) for 4 days in regular growth medium or with mβCD (50 mM) in RPMI–0.2% BSA for 20 min at room temperature (25°C). Cell-associated cholesterol was measured by detaching the cells with 40 mM EDTA in PBS (without calcium and magnesium) at 4°C for up to 40 min. The cells were centrifuged at 1,000 × *g* for 2 min, resuspended in 100 μl of reaction buffer (Amplex Red cholesterol assay kit; Molecular Probes), and homogenized through a 20-gauge needle, followed by measurement of cholesterol using a spectrofluorometer (model 1420 Multilabel Counter; Wallac Victor, Turku, Finland) at 560-nm excitation and 590-nm emission wavelengths according to the manufacturer's conditions and published literature (2). Cholesterol replacement occurred with 0.1 mM water-soluble cholesterol (C-4951; Sigma) in RPMI–0.2% BSA at 37°C for 15 min.

**Fluorescence microscopy.** Cholesterol staining with filipin was performed in HeLa cells fixed with 3% paraformaldehyde for 20 min, washed with PBS and 25 mM ammonium chloride in PBS, and incubated with filipin (100 μg/ml; Sigma) for 2 h at 4°C, following earlier protocols (68). Coverslips were mounted in DAKO fluorescence mounting medium (DAKO Corp., Carpinteria, Calif.) and observed in an upright fluorescence microscope (Polyvar; Merck Corp.) equipped with a 350-nm excitation filter and a 420-nm emission filter. Images were recorded as described previously (18). Confocal laser scanning microscopy (CLSM) was performed on a DM RXA2 TCS SP2 AOBS microscope (Leica Microsystems, Wetzlar, Germany) equipped with an Ar-ArKr laser, a He-Ne 543-594 laser, a He-Ne 633 laser, a diode laser at 405 nm, and a 63× oil immersion objective (N.A. 1.4 PL APO). The pinhole value was 1.0, airy 1, yielding optical sections of ~0.48 μm with a voxel of 0.233 by 0.233 by 0.48 μm. The zoom factor was 2. Image processing was performed with Leica and Photoshop software (Adobe). Quantifications of the fluorescence intensities of Ad2-TR (1 μg of Ad2-TR was used per 12-mm-diameter regular coverslip during cold binding) in different subcellular regions were carried out on complete stacks of optical sections obtained by a far-field fluorescence microscope (Leica DM-IRBE), and deconvolution was done by the Metamorph Software package (Universal Imaging Corp.) as described previously (47).

**Fluid phase endocytosis and flow cytometry.** Fluid phase endocytosis was determined as described previously (39). Briefly, cells were incubated with Ad2 (40 μg/ml) in the cold, washed, and incubated with warm RPMI-BSA for 5 min, followed by a pulse with warm RPMI-BSA containing dextran-fluorescein isothiocyanate (FITC) (1 mg/ml) for 5 min and a chase in the absence of dextran for 5 min. Alternatively, cells were treated with phorbol myristate acetate (PMA; 200 nm) during the dextran pulse or were left unstimulated. After the chase, the cells were washed in cold RPMI-BSA and acid stripped in 0.1 M sodium acetate–0.05 M NaCl (pH 5.5) and detached with trypsin, and at least 10,000 viable cells were analyzed by flow cytometry in an Epics XL sorter (Beckman Coulter, Miami, Fla.). Dextran-FITC release from endosomes was quantitated by visual inspection of cells on glass coverslips using an upright fluorescence microscope (Polyvar; Merck) equipped with 40× optics as described earlier (19). Release-positive cells had a glowing green fluorescent phenotype. Dextran release from endosomes was verified using CLSM as described above. Cell surface CAR and αv integrins were determined by flow cytometry as described previously (45). Briefly, ~$10^6$ cells were detached from the 35-mm-diameter dishes with 20 mM EDTA in PBS for 15 min, washed, and incubated with anti-αv or anti-CAR mouse monoclonal antibody at 4°C for 1 h. After being washed in RPMI-BSA, the cells were incubated with a rabbit anti-mouse immunoglobulin G coupled to phycoerythrin (20 μg/ml) at 4°C for 1 h, washed, resuspended in 0.3 ml of 2% fetal bovine serum in PBS, and analyzed by flow cytometry.

**Transmission electron microscopy (TEM).** After cold binding to Ad2 (80 μg/ml; multiplicity of infection [MOI], 10,000) for 1 h, washing, and internalization as appropriate, cells were fixed in 2% formaldehyde–1.5% glutaraldehyde in 0.1 M sodium cacodylate buffer, pH 7.4 (CaCo) overnight and washed several times in CaCo, followed by postfixation in 1% $OsO_4$ (Electron Microscopy Sciences) and 1.5% potassium ferricyanide ($FeK_3N_6$) in double-distilled $H_2O$ at 4°C for 60 min (modified according to the method of Simionescu and Simionescu [64]). Specimens were rinsed in 0.1 M sodium cacodylate, contrasted with 1% tannic acid in 0.05 M sodium cacodylate at room temperature for 45 min, washed in 1% sodium sulfate, rinsed in $H_2O$, stained in 2% uranylacetate in $H_2O$ overnight, and embedded in Epon as described previously (46). Virus particles were quantified at ×50,000 magnification in ultrathin sections at the plasma

membrane, endosomes, and cytosol viewed in a transmission electron microscope (Zeiss EM 902A) at an acceleration voltage of 80,000 V (46).

**Statistical analyses.** Results were expressed as the mean values from, typically, three experimental samples, including the standard error of the mean and significance calculation by one-sided *t* tests.

## RESULTS

Cholesterol has a key role in organizing sphingolipid rafts that serve as platforms of cell signaling, protein organization, and sorting. Its homeostasis is tightly controlled by spontaneous efflux, synthesis in the endoplasmic reticulum, and receptor-mediated uptake of lipoproteins (38, 65). The rate-limiting enzyme in cholesterol synthesis is 3-hydroxy-3-methylglutaryl coenzyme A reductase, which can be inhibited by LOV (72). Here, we sought to determine the basis of the requirement for cholesterol for infection of epithelial cells with species C Ads.

**Cholesterol reduction inhibits Ad5 gene expression.** Cholesterol levels were assessed in HeLa cells treated for 4 days with LOV, in combination with MEV to ensure cell survival (66). Alternatively, cholesterol was extracted from the plasma membrane by mβCD for 20 min. While the MEV-LOV treatment reduced cholesterol by ~20%, mβCD or mβCD plus MEV-LOV lowered cholesterol by 45 and 55%, respectively, as indicated by Amplex Red quantifications (Fig. 1A). This loss of cholesterol was readily reversed by the addition of cholesterol for 15 min (Fig. 1B). We noticed that the combined application of mβCD and MEV-LOV led to considerable cell stress, i.e., cells started to detach from the glass coverslips. Treatment with mβCD alone, however, had no effect on cell loss and viability, as indicated by the measurement of [$^{35}$S]methionine incorporation into mβCD-treated and control cells (Fig. 1C). In fact, mβCD-treated cells had reduced filipin staining in the cell periphery but not in internal regions compared to control cells, suggesting that peripheral cholesterol had been preferentially reduced, in agreement with the overall cholesterol measurements by Amplex Red (Fig. 1D).

We next measured Ad5-mediated transduction in cells treated with mβCD. mβCD inhibited the expression of CMV promoter-driven *luc* in a dose-dependent manner, maximally fourfold at 25 or 50 mM measured at 4 h p.i. (Fig. 2A). In the presence of 0.05 mM cholesterol, low concentrations of mβCD (<5 mM) had no effect, indicating that the mβCD inhibition was due to cholesterol reduction rather than to nonspecific effects. In the absence of mβCD, cholesterol increased gene expression up to threefold compared to untreated cells, further supporting the notion that cholesterol is important for Ad5-mediated gene expression. The mβCD (50 mM) inhibition was strongest at a high MOI of 1,000 (Fig. 2B), and it persisted for up to 16 h postinfection (p.i.) at a level of at least twofold in cells infected at a lower MOI of 100 (Fig. 2D), similar to an earlier report (3). It was unlikely that mβCD inhibited the CMV promoter, since neither mβCD nor cholesterol affected the CMV-*luc* activity in transiently transfected HeLa cells (Fig. 2C). Surprisingly, restoring the cholesterol levels of mβCD-treated cells did not fully rescue Ad5 transduction (Fig. 2B). Ad5 transduction of both normal and mβCD-treated cells, however, was dependent on αv integrins and CAR, as indicated by 3- and 10-fold inhibition with cRGD peptides and soluble fiber knob, respectively (Fig. 2E). The effect of fiber knob was not enhanced by mβCD, suggesting that knob and

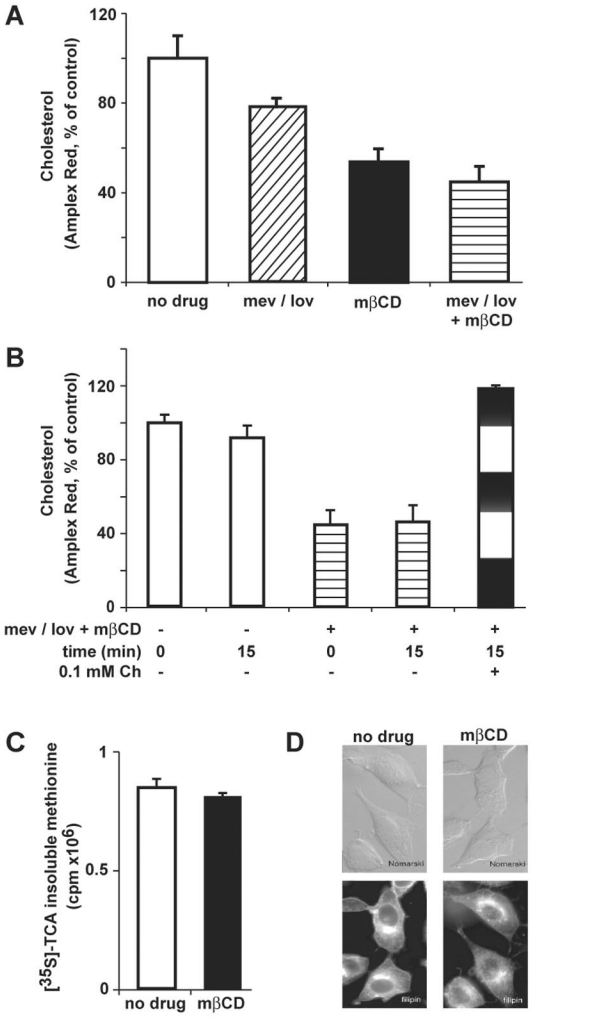


FIG. 1. Reduction of cellular cholesterol by mβCD. (A) Cholesterol was measured enzymatically by determination of cholesterol oxidase activity using an Amplex Red readout in HeLa cells incubated with the cholesterol synthesis inhibitor LOV plus MEV or mβCD. (B) MEV-LOV- plus mβCD-treated cells were refilled with 0.1 mM cholesterol (Ch) for 15 min, followed by Amplex Red measurement. (C) Biosynthetic activity of control and mβCD-treated cells by determination of [$^{35}$S]methionine incorporation, showing the mean values of three samples from one representative experiment. (D) Filipin staining of control and mβCD-treated cells, including Nomarski images (top). The error bars indicate the corresponding standard errors of the mean.

cholesterol were acting at the same point, e.g., CAR localized in cholesterol raft domains. Accordingly, the function blocking anti-CAR antibody E1-1 inhibited $^{35}$S-Ad2 binding to control cells, mβCD-treated cells, and cells with cholesterol replaced to similar extents (Fig. 3A). Note that the apparent reduction of virus binding to mβCD-treated cells had low statistical significance compared to binding to control cells ($P > 0.05$; *t* test). In contrast, the inhibition of gene expression by cRGD peptides was additive to the mβCD inhibition, suggesting that RGD-binding integrins accessed by Ad5 perhaps occur in both raft and nonraft domains (Fig. 2E). Importantly, αv integrins were readily detectable in both normal and cholesterol-re-

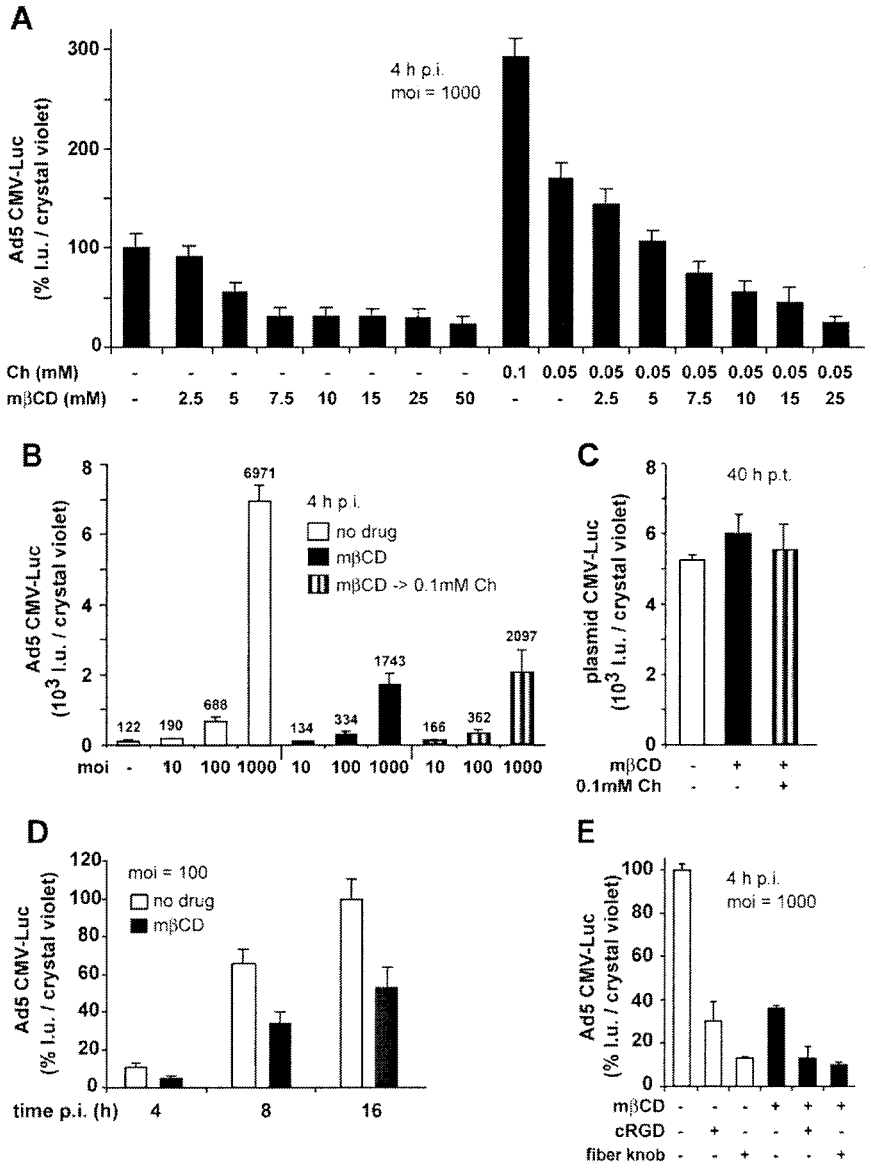


FIG. 2. Ad5-mediated gene delivery, but not plasmid DNA, is affected by cholesterol depletion and replacement. HeLa cell were incubated with cholesterol (Ch), mβCD, or mβCD followed by cholesterol replacement (mβCD → 0.1mM Ch). Ad5-Luc was bound in the cold, and the cells were washed as described in Materials and Methods. The results are expressed as luciferase light units (l.u.) normalized to the corresponding cell numbers obtained by crystal violet measurements of parallel samples. (A) Dose dependence of mβCD and cholesterol treatments 4 h p.i. (B) Cholesterol depletion affects Ad5-Luc gene expression at different MOIs 4 h p.i. (C) Lack of effect of cholesterol depletion on luciferase expression of plasmid DNA in cells treated with mβCD or cholesterol 8 h posttransfection (p.t.) and assayed for luciferase expression 40 h p.t. (D) Time course of Ad5-Luc gene expression in control and cholesterol-depleted cells. (E) Fiber knob and cRGD peptides inhibit Ad5-Luc gene expression in control and cholesterol-depleted cells 4 h p.i. −, not present; +, present. The error bars indicate the corresponding standard errors of the mean.

duced cells, using a function-blocking anti-αv integrin antibody, despite a small reduction by ~25% upon mβCD treatment (Fig. 3B). These results reinforce the notion that the cellular cholesterol balance is critical for Ad transduction.

**Ad2 endocytosis requires cholesterol.** We next analyzed viral endocytosis in mβCD-treated and control cells using quantitative TEM. At 15 min p.i., 13% of the viral particles were found in endosomes, 25% in the cytosol, and ~60% at the plasma membranes of control cells (Fig. 4A and B). This corresponded well with biochemical internalization assays using surface trypsinizations at low MOIs (21), confirming the validity of the high-MOI EM approach. This in situ analysis was necessary, since trypsinization of mβCD-treated cells caused severe cell damage (not shown). In contrast to control cells, Ad2 internalization was strongly inhibited in the cholesterol-reduced cells, with only a few percent of the particles in endosomes and in the cytosol (Fig. 4A and B). About 80% or more of the plasma membrane-associated virus particles of control and

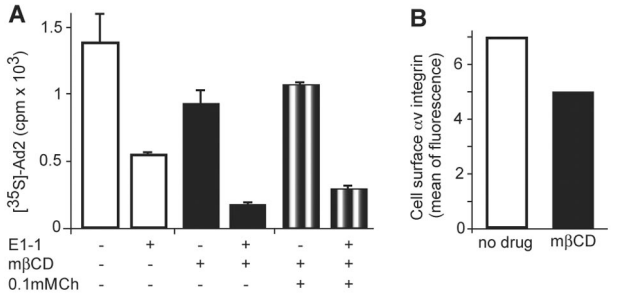


FIG. 3. Ad2 binding to normal and cholesterol-depleted cells depends on CAR. (A) HeLa cells were treated with mβCD, and cholesterol (Ch) was replaced. The cells were incubated with the anti-CAR antibody E1-1 and [$^{35}$S]methionine-labeled Ad2 in the cold and examined for cell-associated virus by liquid scintillation counting. (B) Control and mβCD-treated cells were examined for cell surface αv integrins by flow cytometry using the function-blocking 17E6 antibody and secondary phycoerythrin-conjugated antibodies. The results are expressed as means of fluorescence. −, not present; +, present. The error bars indicate the corresponding standard errors of the mean.

mβCD-treated cells were localized in smooth regions, and ~18 and 13% were in plasma membrane lattices, i.e., electron-dense flat domains associated with clathrin (Fig. 4C) (69). About 3 and 1% of the plasma membrane-associated particles were in coated pits of control and mβCD-treated cells, respectively. The levels of coated-pit-associated virus that were recovered in cholesterol-replaced cells were similar to those of control cells. These results are consistent with the notion that cholesterol depletion blocks clathrin-mediated endocytosis of Ad2. Cholesterol replacement, in turn, restored virus localization to clathrin-coated pits, allowing virus internalization (Fig. 4).

**Macropinocytosis and Ad2 delivery to the cytosol depend on cholesterol.** Ad2 triggers the formation of macropinosomes and the delivery of fluid phase contents into the cytosol, which is due to virus-induced macropinosomal leakage (39). Using flow cytometry, we found that the Ad2-induced fluid phase endocytosis of 10-kDa dextran labeled with FITC was completely blocked in mβCD-treated cells, similar to PMA-induced fluid phase endocytosis (Fig. 5A) and consistent with an earlier report demonstrating cholesterol dependence of growth

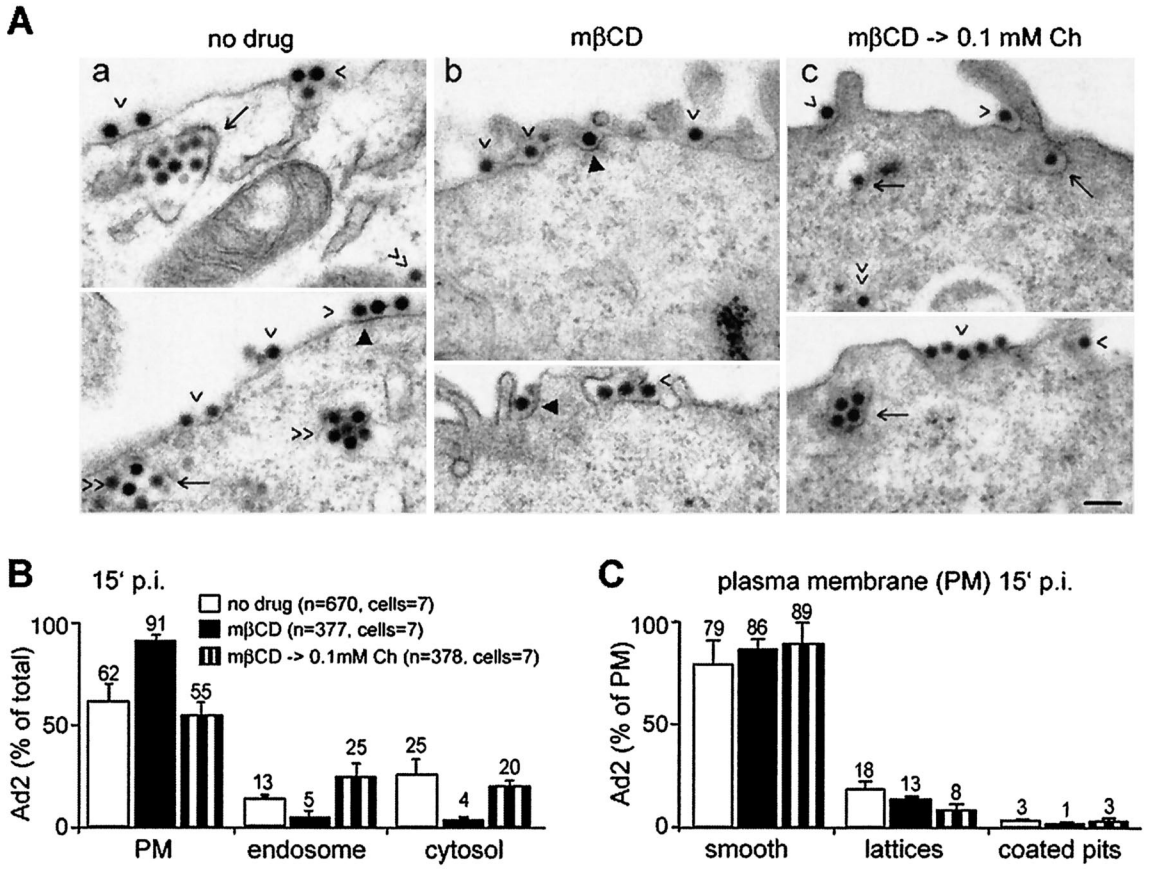


FIG. 4. Ad2 endocytosis is inhibited in cholesterol-depleted cells. (A) Ad2 was bound to control cells, mβCD-treated cells, or mβCD-treated cells with cholesterol replaced (mβCD → 0.1mM Ch) and was internalized for 15 min, fixed, and prepared for TEM analysis. The arrowheads indicate plasma membrane-associated virus, the arrows indicate endosomal virus, the double arrowheads indicate cytosolic virus, and the solid arrowheads point out Ad2 particles at clathrin lattices (69). (B) Quantitative analyses of Ad2 at the plasma membrane (PM), in endosomes, and in the cytosol expressed as percentages of total particles, with n representing the number of Ad2 particles analyzed. (C) Analyses of Ad2 in smooth plasma membrane regions, in clathrin lattices, and in coated pits expressed as percentages of plasma membrane-associated particles. The error bars indicate the corresponding standard errors of the mean.

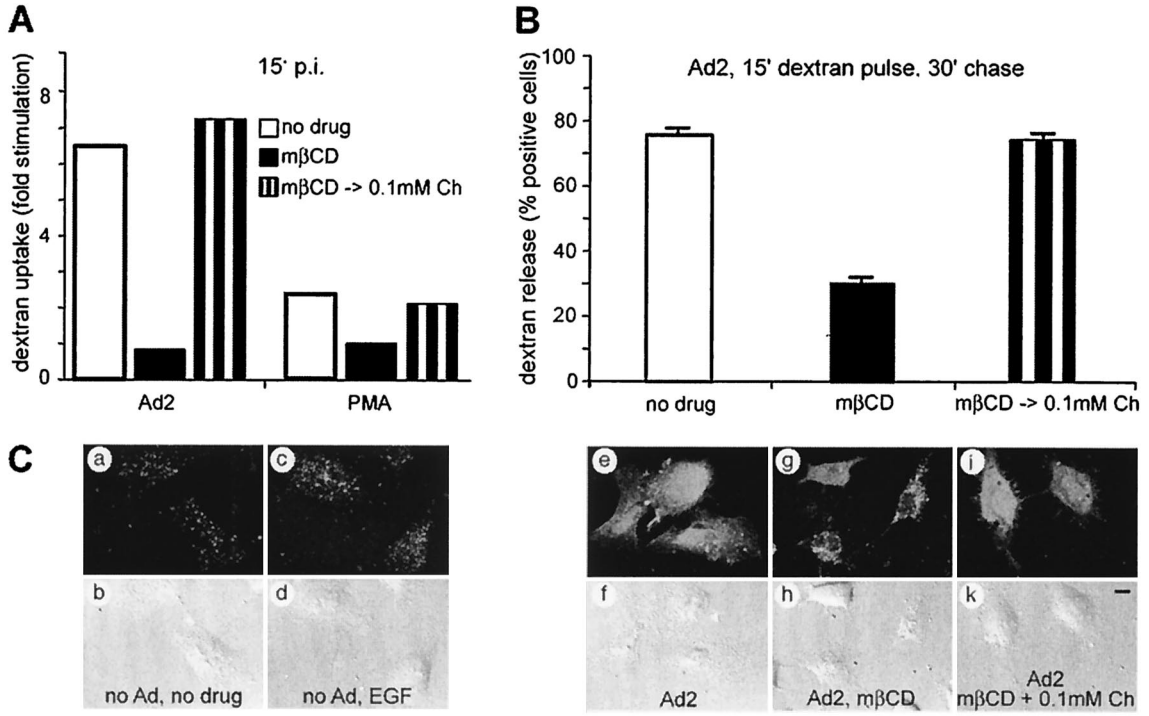


FIG. 5. Cholesterol-dependent Ad2-stimulated macropinocytosis and delivery of fluid phase endosomal contents to the cytosol. (A) Control cells, mβCD-treated cells, or mβCD-treated cells with cholesterol replaced (mβCD → 0.1mM Ch) were incubated with Ad2 in the cold, washed, internalized at 37°C in the presence of dextran-FITC for 15 min, and analyzed by flow cytometry. (B) The internalized dextran was compared to the dextran internalization in PMA-treated cells and was normalized to uninfected, unstimulated cells. Dextran release to the cytosol of cells pulsed with dextran-FITC for 15 min and chased in the absence of dextran for 30 min was analyzed by fluorescence microscopy, and the number of cells with dextran-positive nuclei was determined. (C) Examples of control cells containing endosomal dextran (punctate signals [a, c, and g]) and cytosolic dextran (e and i) were imaged by CLSM, and total projections are shown, including the corresponding Nomarski images (b, d, f, h, and k). Bar = 10 μm. The error bars indicate the corresponding standard errors of the mean.

factor-activated macropinocytosis (23). The Ad2- and PMA-induced dextran uptake could be readily restored by cholesterol replacement. We then investigated whether dextran was delivered into the cytosol by using fluorescence microscopy of single cells. The results indicated that >75% of the Ad2-infected cells contained cytosolic dextran-FITC, as indicated by strong homogeneous fluorescence across the cytoplasm and the nucleus (Fig. 5B and C). Uninfected cells or epidermal growth factor-activated cells had punctate cytoplasmic dextran fluorescence but no intranuclear signals. Likewise, ~70% of the Ad2- and mβCD-treated cells were lacking nuclear dextran-FITC. Dextran delivery to the cytosol could be completely restored in cells with cholesterol replaced, indicating that Ad2-induced macropinosomal leakage was restored.

Next, we analyzed the delivery of Ad2 particles from endosomes to the cytosol in quantitative EM experiments at 70 min p.i. In control cells, >80% of the cell-associated Ad2 was in the cytosol, 7% was on the plasma membrane, and 11% was in endosomes (Fig. 6A). In contrast, mβCD-treated cells had 50% less cytosolic Ad2 than control cells (Fig. 6B). Very few particles were found at the nuclear membrane, unlike in control cells (not shown). More than 40% of the particles were left at the plasma membrane, and only 15% were in endosomes, confirming that cholesterol depletion inhibited viral endocytosis. As expected, the numbers of cytosolic particles at the plasma membrane were low in cells with cholesterol replaced (12%), but surprisingly, the endosomal levels were as high as 47% and the cytosolic particles remained at 41%, similar to the cells without cholesterol replacement (Fig. 6C). Interestingly, most of the endosomal Ad2 was found in large vesicles that were often multivesiculated, consistent with late endosomes or lysosomes. These results indicated that cholesterol replacement restored Ad2 endocytosis but failed to efficiently deliver particles to the cytosol. We also analyzed whether the uptake of ts1, a mutant Ad2 that is inhibited at endosomal escape (20, 78), is cholesterol dependent. ts1 bears a point mutation in the viral protease which blocks the processing of at least three viral capsid proteins and three core proteins. ts1 was found to be endocytosed efficiently in control cells, leaving 3% of the particles at the plasma membrane and 70% in predominantly large endosomes (Fig. 6D). This was in good agreement with biochemical measurements of internalization and lysosomal degradation, the latter being sensitive to the treatment of cells with leupeptin, an inhibitor of acid proteases (20). In mβCD-treated cells, ts1 internalization was somewhat inhibited, leaving 18% of the particles at the plasma membrane (Fig. 6E). The effect, however, was ~3-fold less prominent than with wild-type (wt) Ad2, suggesting that ts1 might internalize on a pathway that is rather insensitive to cholesterol depletion. ts1 binds CAR and is internalized in an RGD peptide-sensitive

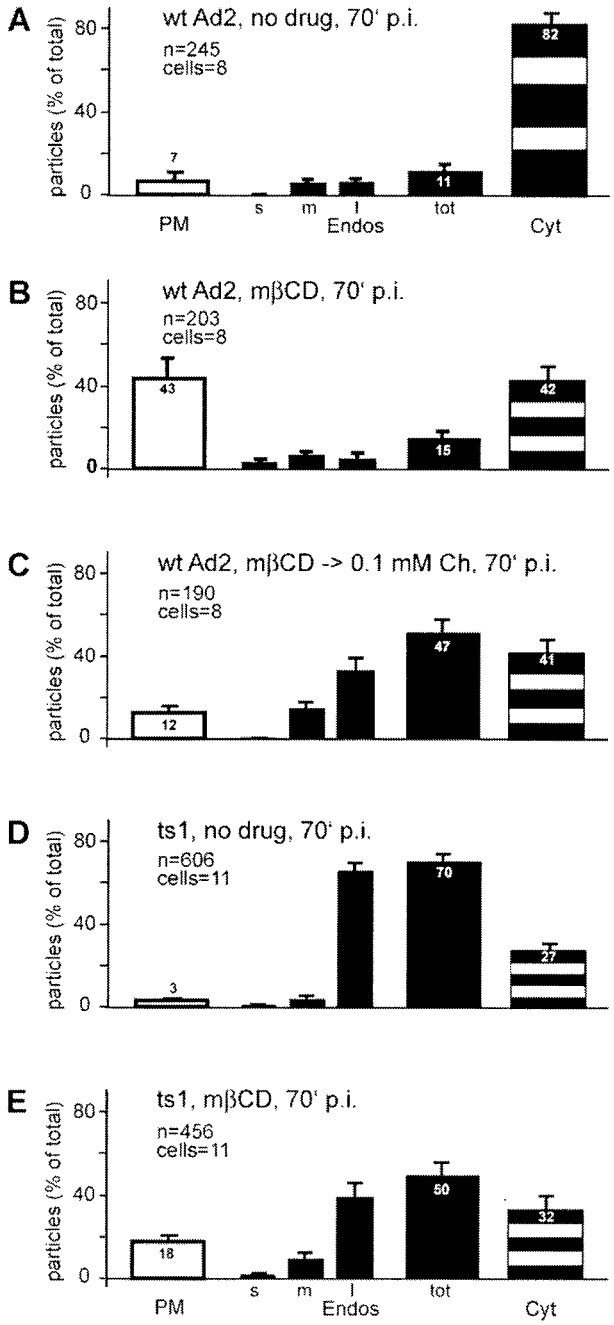


FIG. 6. Cholesterol depletion inhibits endosomal escape of Ad2 but does not affect endocytosis of ts1. wt Ad2 or ts1 Ad2 was bound to control HeLa cells, mβCD-treated HeLa cells, or mβCD-treated HeLa cells with cholesterol replaced (mβCD → 0.1mM Ch) in the cold, internalized for 70 min, and analyzed by TEM. Virus particles at the plasma membrane (PM), in endosomes (endos), and in the cytosol (Cyt) were quantitated as described in the legend to Fig. 4. The analysis of total endosomal virus (tot) included the determination of particles in small endosomes (s; <150-nm diameter), medium-size endosomes (m; ~300-nm diameter), and large multivesicular endosomes (l;, >300-nm diameter). The error bars indicate the corresponding standard errors of the mean.

manner (20), albeit without cell activation (70). This pathway may be similar to the uptake of low levels of wild-type Ad2 in cholesterol-depleted cells (Fig. 6).

We also measured cytoplasmic transport of incoming Ad2 labeled with TR in control and cholesterol-depleted cells, using quantitative fluorescence microscopy. This approach gives good indirect indications of endosomal escape of Ad2, as shown in the case of the endosomal ts1, which is not delivered to the nuclear region, unlike wt Ad2 (47). Cells treated with mβCD or with MEV-LOV plus mβCD accumulated significantly fewer Ad2 particles in the nuclear and perinuclear regions than control cells (Fig. 7 and data not shown), in agreement with defective viral escape from endosomes. Cholesterol replacement in turn had no effect at 90 min p.i. and partially rescued nuclear targeting of Ad2-TR at 135 min p.i. (not shown). These measurements confirmed that cholesterol is required for efficient entry and nuclear targeting of Ad2 in epithelial cells.

## DISCUSSION

Many ways lead into a cell, but specific pathways elicit pathogen infection of particular cell types. Here, we have shown that endocytosis and endosomal escape of species C Ad2 and Ad5 in epithelial cells require cholesterol. In normal cells, Ad2 rapidly enters through the clathrin pathway, leading to viral-gene expression (39). Supplementing the normal growth medium with cholesterol was shown here to further enhance Ad5 transgene expression. In contrast, cells depleted of cholesterol internalized Ad by a slow and inefficient pathway, with limited particle delivery to the cytosol. Cholesterol depletion also affected Ad5 gene expression, depending on the virus dose, with inhibitions of 29, 51, and 75% at MOIs of 10, 100, and 1,000, respectively. This differential requirement for cholesterol could be due to different entry pathways at low and high MOIs. Alternatively, it is possible that the low levels of cellular cholesterol after mβCD treatment suffice for virus uptake and infection at low MOIs but become limiting at high MOIs. The slow uptake of high-MOI Ad2 in cholesterol-reduced cells is similar to the internalization of anthrax toxin, which oligomerizes in lipid rafts and is internalized by rapid clathrin-mediated endocytosis, whereas monomeric toxin is internalized slowly (1). Furthermore, the slow cholesterol-independent entry path of Ad2 resembles the uptake of the Ad2 ts1 mutant in normal cells. ts1 is defective at endosomal escape, cycles between endosomes and the plasma membrane, and is degraded in lysosomes (20). Its uptake is CAR and integrin dependent but cholesterol independent.

Recently, CAR has been colocalized with the glycosphingolipid GM1 labeled with cholera toxin B subunit in cholesterol-rich membrane domains, distinct from caveolin domains (3, 52). Although it is not known if CAR is endocytosed, it has been suggested that CAR is in a network of proteins and specialized lipids that may undergo endocytosis, depending on the intactness of the domain, extracellular ligands, or intracellular activation. Likewise, the integrin coreceptors can be localized to lipid rafts, e.g., upon activation, as shown for the leukocyte-associated LFA-1 (αLβ2) integrin (26). It is unclear, however, if integrins directly associate with rafts, since they lack the palmitoyl modifications typical of many raft- and

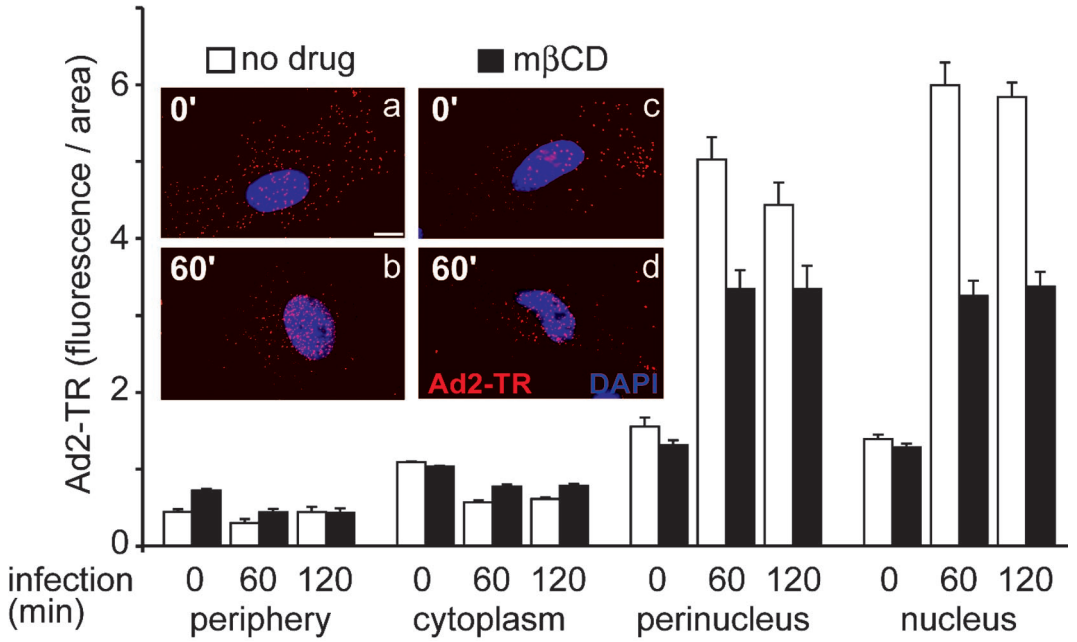


FIG. 7. Nuclear targeting of Ad2-TR is inhibited in cholesterol-depleted cells. Ad2-TR was bound to control or mβCD-treated HeLa cells in the cold and internalized for different times as indicated. The cells were fixed, and the subcellular distribution of Ad2-TR was determined by quantitative microscopy. The results are expressed as fluorescence per unit area. Representative examples of cells fixed at 0 and 60 min p.i. are shown in the inset. The nuclei are stained with 4,6-diamidino-2-phenylindole (blue). Bar = 10 μm. The error bars indicate the corresponding standard errors of the mean.

sphingolipid-associated proteins. Possibly, integrins localize to rafts indirectly, as shown, e.g., for αvβ3 integrin complexed with tetraspanning and integrin-associated proteins (22). Thus, cholesterol extraction from the plasma membrane is likely to disturb the organization of lipid rafts necessary for efficient CAR- and integrin-dependent entry of Ad2.

Typically, cholesterol depletion blocks caveolar endocytosis and the uptake of other lipid raft-enriched plasma membrane domains (55), consistent with the notion that some lipid raft markers can be internalized without clathrin-coated pits (50). Other markers, such as analogues of sphingomyelin, however, are taken up approximately equally by clathrin-dependent and -independent pathways (57). Further studies have shown that clathrin-coated vesicles, and by inference clathrin-coated pits, contain cholesterol, indistinguishable from other plasma membrane regions (68). In fact, clathrin-mediated endocytosis of transferrin receptor and epidermal growth factor receptor is inhibited in cholesterol-depleted cells without affecting back trafficking of the receptor to the surface (58, 69). The observation that flat coated membranes accumulate in mβCD-treated cells suggested that cholesterol is needed to induce curvature of the membrane and detachment of coated pits from the surface. Consistent with this observation, we have found that wt Ad2 localized threefold less frequently to coated pits in cholesterol-depleted cells than in control cells or cells with cholesterol replaced. The coated pits that we observed in the cholesterol-depleted cells appeared to be of regular shape. Together, these results support the notion that the rapid clathrin-mediated Ad2 endocytosis requires cholesterol. Whether it requires additional raft components is unknown. These results are similar to a recent report on the minor receptor group using human rhinovirus 2, which enters cells in a cholesterol-, dynamin-, amphiphysin-, and AP180-dependent manner, indicative of the clathrin-coated-pit pathway (67). The slow cholesterol-independent endocytic pathway of Ad2, in turn, may be independent of clathrin. Accordingly, Ad particles infecting CAR-expressing epithelial cells were found in both clathrin-associated and non-clathrin-associated membranes (3, 21, 46), although the clathrin-associated pathway leads to infection (39, 75). This supports the notion that Ad2 can use multiple pathways into the cell and that in undisturbed cells the clathrin pathway predominates over the other entry pathways.

Besides using clathrin-mediated endocytosis and a slow cholesterol-independent entry pathway, incoming species C Ads activate macropinocytosis (39). Macropinocytosis is independent of dominant-negative dynamin K44A and is blocked by protein kinase C inhibitors and the sodium-proton exchange inhibitor amiloride. It is not required for Ad2 internalization, and it releases fluid phase contents into the cytosol when virus escapes from endosomes (39, 46). Macropinocytosis was not observed in cholesterol-depleted cells, and no fluid phase markers were delivered to the cytosol in the presence of Ad2, consistent with the earlier notion that growth factor-activated macropinocytosis is cholesterol dependent (23). Cholesterol repletion readily restored the rapid Ad2 endocytosis and macropinocytosis, and also the release of macropinosomal contents to the cytosol, but it did not restore viral escape from endosomes and gene expression. The depletion of cholesterol several hours before infection, followed by washout of the drug, however, has no effect on Ad5 transduction (3). Likewise, the addition of extra cholesterol to control cells even enhanced viral-gene expression. It is possible that the acute supply of

cholesterol to the depleted cells affected the proper lipid organization necessary for viral escape from endosomes (38). Cholesterol replacement may not entirely restore the functionality of Ad-containing endosomes. Likewise, intracellular-membrane trafficking may be altered in the restored cells. This is based on the observation that an excess of cholesterol can be transported from the plasma membrane to the endoplasmic reticulum, where cholesterol becomes esterified for storage in cytoplasmic lipid droplets (28). Alternatively, cholesterol depletion and replacement may alter the selection of the endocytic pathway that the virus takes in normal cells, namely, the rapid clathrin pathway and, as a less efficient alternative, a cholesterol-independent pathway. This possibility has recently been illustrated for the transforming growth factor β receptor, which can be internalized by either a clathrin- or raft-dependent pathway (11). The clathrin pathway leads the transforming growth factor β receptor into signaling endosomes, whereas the raft pathway accelerates receptor degradation. Accordingly, Ad2 might be taken up through the clathrin pathway to signaling plasma membrane domains or endosomes, facilitating the proper execution of endosomal escape.

## ACKNOWLEDGMENTS

We thank Simon Goodman (Merck) for the 17E6 antibody, Dominique Sirena (University of Zürich) for gifts of plasmid DNA, and Mark Marsh (University College London) and all members of the laboratory for stimulating discussions.

This work was supported by funds from the Swiss National Science Foundation and the Kanton Zürich (U.F.G.).

## REFERENCES

1. **Abrami, L., S. Liu, P. Cosson, S. H. Leppla, and F. G. van der Goot.** 2003. Anthrax toxin triggers endocytosis of its receptor via a lipid raft-mediated clathrin-dependent process. J. Cell Biol. **160:**321–328.
2. **Amundson, D. M., and M. Zhou.** 1999. Fluorometric method for the enzymatic determination of cholesterol. J. Biochem. Biophys. Methods **38:**43–52.
3. **Ashbourne Excoffon, K. J., T. Moninger, and J. Zabner.** 2003. The coxsackie B virus and adenovirus receptor resides in a distinct membrane microdomain. J. Virol. **77:**2559–2567.
4. **Bantel-Schaal, U., B. Hub, and J. Kartenbeck.** 2002. Endocytosis of adeno-associated virus type 5 leads to accumulation of virus particles in the Golgi compartment. J. Virol. **76:**2340–2349.
5. **Bella, J., and M. G. Rossmann.** 1999. Rhinoviruses and their ICAM receptors. J. Struct. Biol. **128:**69–74.
6. **Bousarghin, L., A. Touze, P. Y. Sizaret, and P. Coursaget.** 2003. Human papillomavirus types 16, 31, and 58 use different endocytosis pathways to enter cells. J. Virol. **77:**3846–3850.
7. **Chardonnet, Y., and S. Dales.** 1970. Early events in the interaction of adenoviruses with HeLa cells. I. Penetration of type 5 and intracellular release of the DNA genome. Virology **40:**462–477.
8. **Chazal, N., and D. Gerlier.** 2003. Virus entry, assembly, budding, and membrane rafts. Microbiol. Mol. Biol. Rev. **67:**226–237.
9. **Conner, S. D., and S. L. Schmid.** 2003. Regulated portals of entry into the cell. Nature **422:**37–44.
10. **Damke, H., T. Baba, D. E. Warnock, and S. L. Schmid.** 1994. Induction of mutant dynamin specifically blocks endocytic coated vesicle formation. J. Cell Biol. **127:**915–934.
11. **Di Guglielmo, G. M., C. Le Roy, A. F. Goodfellow, and J. L. Wrana.** 2003. Distinct endocytic pathways regulate TGF-beta receptor signalling and turnover. Nat. Cell Biol. **5:**410–421.
12. **Doxsey, S. J., F. M. Brodsky, G. S. Blank, and A. Helenius.** 1987. Inhibition of endocytosis by anti-clathrin antibodies. Cell **50:**453–463.
13. **Ebbinghaus, C., A. Al-Jaibaji, E. Operschall, A. Schoeffel, I. Peter, U. F. Greber, and S. Hemmi.** 2001. Functional and selective targeting of adenovirus to high affinity Fcg receptor I positive cells using a bispecific hybrid adaptor. J. Virol. **75:**480–489.
14. **Fausch, S. C., D. M. Da Silva, and W. M. Kast.** 2003. Differential uptake and cross-presentation of human papillomavirus virus-like particles by dendritic cells and Langerhans cells. Cancer Res. **63:**3478–3482.
15. **Felberbaum-Corti, M., F. G. Van Der Goot, and J. Gruenberg.** 2003. Sliding doors: clathrin-coated pits or caveolae? Nat. Cell Biol. **5:**382–384.
16. **FitzGerald, D. J. P., R. Padmanabhan, I. Pastan, and M. C. Willingham.** 1983. Adenovirus-induced release of epidermal growth factor and *Pseudomonas* toxin into the cytosol of KB cells during receptor mediated endocytosis. Cell **32:**607–617.
17. **Gaggar, A., D. M. Shayakhmetov, and A. Lieber.** 2003. CD46 is a cellular receptor for group B adenoviruses. Nat. Med. **9:**1408–1412.
18. **Greber, U. F., M. Y. Nakano, and M. Suomalainen.** 1998. Adenovirus entry into cells: a quantitative fluorescence microscopy approach, p. 217–230. *In* W. S. M. Wold (ed.), Adenovirus methods and protocols. Humana Press, Inc., Totowa, N.J.
19. **Greber, U. F., M. Suomalainen, R. P. Stidwill, K. Boucke, M. Ebersold, and A. Helenius.** 1997. The role of the nuclear pore complex in adenovirus DNA entry. EMBO J. **16:**5998–6007.
20. **Greber, U. F., P. Webster, J. Weber, and A. Helenius.** 1996. The role of the adenovirus protease in virus entry into cells. EMBO J. **15:**1766–1777.
21. **Greber, U. F., M. Willetts, P. Webster, and A. Helenius.** 1993. Stepwise dismantling of adenovirus 2 during entry into cells. Cell **75:**477–486.
22. **Green, J. M., A. Zhelesnyak, J. Chung, F. P. Lindberg, M. Sarfati, W. A. Frazier, and E. J. Brown.** 1999. Role of cholesterol in formation and function of a signaling complex involving αvβ3, integrin-associated protein (CD47), and heterotrimeric G proteins. J. Cell Biol. **146:**673–682.
23. **Grimmer, S., B. van Deurs, and K. Sandvig.** 2002. Membrane ruffling and macropinocytosis in A431 cells require cholesterol. J. Cell Sci. **115:**2953–2962.
24. **Helenius, A., J. Kartenbeck, K. Simons, and E. Fries.** 1980. On the entry of Semliki Forest virus into BHK-21 cells. J. Cell Biol. **84:**404–420.
25. **Hewlett, L. J., A. R. Prescott, and C. Watts.** 1994. The coated pit and macropinocytic pathways serve distinct endosome populations. J. Cell Biol. **124:**689–703.
26. **Hogg, N., R. Henderson, B. Leitinger, A. McDowall, J. Porter, and P. Stanley.** 2002. Mechanisms contributing to the activity of integrins on leukocytes. Immunol. Rev. **186:**164–171.
27. **Hogle, J. M.** 2002. Poliovirus cell entry: common structural themes in viral cell entry pathways. Annu. Rev. Microbiol. **56:**677–702.
28. **Ioannou, Y. A.** 2001. Multidrug permeases and subcellular cholesterol transport. Nat. Rev. Mol. Cell Biol. **2:**657–668.
29. **Jin, M., J. Park, S. Lee, B. Park, J. Shin, K. J. Song, T. I. Ahn, S. Y. Hwang, B. Y. Ahn, and K. Ahn.** 2002. Hantaan virus enters cells by clathrin-dependent receptor-mediated endocytosis. Virology **294:**60–69.
30. **Johannes, L., and C. Lamaze.** 2002. Clathrin-dependent or not: is it still the question? Traffic **3:**443–451.
31. **Lafer, E. M.** 2002. Clathrin-protein interactions. Traffic **3:**513–520.
32. **Lafont, F., G. Tran Van Nhieu, K. Hanada, P. Sansonetti, and F. G. van der Goot.** 2002. Initial steps of Shigella infection depend on the cholesterol/sphingolipid raft-mediated CD44-IpaB interaction. EMBO J. **21:**4449–4457.
33. **Lamaze, C., A. Dujeancourt, T. Baba, C. G. Lo, A. Benmerah, and A. Dautry-Varsat.** 2001. Interleukin 2 receptors and detergent-resistant membrane domains define a clathrin-independent endocytic pathway. Mol. Cell **7:**661–671.
34. **Liu, N. Q., A. S. Lossinsky, W. Popik, X. Li, C. Gujuluva, B. Kriederman, J. Roberts, T. Pushkarsky, M. Bukrinsky, M. Witte, M. Weinand, and M. Fiala.** 2002. Human immunodeficiency virus type 1 enters brain microvascular endothelia by macropinocytosis dependent on lipid rafts and the mitogen-activated protein kinase signaling pathway. J. Virol. **76:**6689–6700.
35. **Mabit, H., M. Y. Nakano, U. Prank, B. Saam, K. Döhner, B. Sodeik, and U. F. Greber.** 2002. Intact microtubules support adenovirus and herpes simplex virus infections. J. Virol. **76:**9962–9971.
36. **Marsh, M., and A. Pelchen-Matthews.** 2000. Endocytosis in viral replication. Traffic **1:**525–532.
37. **Matlin, K. S., H. Reggio, A. Helenius, and K. Simons.** 1982. Infectious entry pathway of influenza virus in a canine kidney cell line. J. Cell Biol. **91:**601–613.
38. **Maxfield, F. R., and D. Wustner.** 2002. Intracellular cholesterol transport. J. Clin. Investig. **110:**891–898.
39. **Meier, O., K. Boucke, S. Vig, S. Keller, R. P. Stidwill, S. Hemmi, and U. F. Greber.** 2002. Adenovirus triggers macropinocytosis and endosomal leakage together with its clathrin mediated uptake. J. Cell Biol. **158:**1119–1131.
40. **Meier, O., and U. F. Greber.** 2003. Adenovirus endocytosis. J. Gene Med. **5:**451–462.
41. **Mitjans, F., D. Sander, J. Adan, A. Sutter, J. M. Martinez, C. S. Jaggle, J. M. Moyano, H. G. Kreysch, J. Piulats, and S. L. Goodman.** 1995. An anti-alpha v-integrin antibody that blocks integrin function inhibits the development of a human melanoma in nude mice. J. Cell Sci. **108:**2825–2838.
42. **Morgan, C., H. S. Rosenkranz, and B. Mednis.** 1969. Structure and development of viruses as observed in the electron microscope. X. Entry and uncoating of adenovirus. J. Virol. **4:**777–796.
43. **Muro, S., R. Wiewrodt, A. Thomas, L. Koniaris, S. M. Albelda, V. R. Muzykantov, and M. Koval.** 2003. A novel endocytic pathway induced by clustering endothelial ICAM-1 or PECAM-1. J. Cell Sci. **116:**1599–1609.
44. **Nabi, I. R., and P. U. Le.** 2003. Caveolae/raft-dependent endocytosis. J. Cell Biol. **161:**673–677.
45. **Nagel, H., S. Maag, A. Tassis, F. O. Nestle, U. F. Greber, and S. Hemmi.** 2003. The αvβ5 integrin of hematopoietic and nonhematopoietic cells is a

transduction receptor of RGD-4C fiber-modified adenoviruses. Gene Ther. **10:**1643–1653.
46. **Nakano, M. Y., K. Boucke, M. Suomalainen, R. P. Stidwill, and U. F. Greber.** 2000. The first step of adenovirus type 2 disassembly occurs at the cell surface, independently of endocytosis and escape to the cytosol. J. Virol. **74:**7085–7095.
47. **Nakano, M. Y., and U. F. Greber.** 2000. Quantitative microscopy of fluorescent adenovirus entry. J. Struct. Biol. **129:**57–68.
48. **Nemerow, G. R., and P. L. Stewart.** 1999. Role of alpha(v) integrins in adenovirus cell entry and gene delivery. Microbiol. Mol. Biol. Rev. **63:**725–734.
49. **Nhieu, G. T., and P. J. Sansonetti.** 1999. Mechanism of Shigella entry into epithelial cells. Curr. Opin. Microbiol. **2:**51–55.
50. **Nichols, B. J.** 2003. GM1-containing lipid rafts are depleted within clathrin-coated pits. Curr. Biol. **13:**686–690.
51. **Nichols, B. J., and J. Lippincott-Schwartz.** 2001. Endocytosis without clathrin coats. Trends Cell Biol. **11:**406–412.
52. **Nusrat, A., C. A. Parkos, P. Verkade, C. S. Foley, T. W. Liang, W. Innis-Whitehouse, K. K. Eastburn, and J. L. Madara.** 2000. Tight junctions are membrane microdomains. J. Cell Sci. **113:**1771–1781.
53. **Ojcius, D. M., Y. Bravo de Alba, J. M. Kanellopoulos, R. A. Hawkins, K. A. Kelly, R. G. Rank, and A. Dautry-Varsat.** 1998. Internalization of Chlamydia by dendritic cells and stimulation of Chlamydia-specific T cells. J. Immunol. **160:**1297–1303.
54. **Parker, J. S. L., W. J. Murphy, D. Wang, S. J. O'Brien, and C. R. Parrish.** 2001. Canine and feline parvoviruses can use human or feline transferrin receptors to bind, enter, and infect cells. J. Virol. **75:**3896–3902.
55. **Pelkmans, L., and A. Helenius.** 2003. Insider information: what viruses tell us about endocytosis. Curr. Opin. Cell Biol. **15:**414–422.
56. **Pieters, J.** 2001. Entry and survival of pathogenic mycobacteria in macrophages. Microbes Infect. **3:**249–255.
57. **Puri, V., R. Watanabe, R. D. Singh, M. Dominguez, J. C. Brown, C. L. Wheatley, D. L. Marks, and R. E. Pagano.** 2001. Clathrin-dependent and -independent internalization of plasma membrane sphingolipids initiates two Golgi targeting pathways. J. Cell Biol. **154:**535–547.
58. **Rodal, S. K., G. Skretting, O. Garred, F. Vilhardt, B. van Deurs, and K. Sandvig.** 1999. Extraction of cholesterol with methyl-beta-cyclodextrin perturbs formation of clathrin-coated endocytic vesicles. Mol. Biol. Cell **10:**961–974.
59. **Roelvink, P. W., A. Lizonova, J. G. M. Lee, Y. Li, J. M. Bergelson, R. W. Finberg, D. E. Brough, I. Kovesdi, and T. J. Wickham.** 1998. The coxsackievirus-adenovirus receptor protein can function as a cellular attachment protein for adenovirus serotypes from subgroups A, C, D, E, and F. J. Virol. **72:**7909–7915.
60. **Rosenberger, C. M., and B. B. Finlay.** 2003. Phagocyte sabotage: disruption of macrophage signalling by bacterial pathogens. Nat. Rev. Mol. Cell. Biol. **4:**385–396.
61. **Russell, D. G., and M. Marsh.** 2001. Endocytosis in pathogen entry and replication, p. 247–280. *In* M. Marsh (ed.), Endocytosis. Oxford University Press, Oxford, United Kingdom.
62. **Segerman, A., J. P. Atkinson, M. Marttila, V. Dennerquist, G. Wadell, and N. Arnberg.** 2003. Adenovirus type 11 uses CD46 as a cellular receptor. J. Virol. **77:**9183–9191.
63. **Sieczkarski, S. B., and G. R. Whittaker.** 2002. Influenza virus can enter and infect cells in the absence of clathrin-mediated endocytosis. J. Virol. **76:**10455–10464.
64. **Simionescu, N., and M. Simionescu.** 1976. Galloylglucoses of low molecular weight as mordant in electron microscopy. I. Procedure, and evidence for mordanting effect. J. Cell Biol. **70:**608–621.
65. **Simons, K., and E. Ikonen.** 2000. How cells handle cholesterol. Science **290:**1721–1726.
66. **Simons, M., P. Keller, B. De Strooper, K. Beyreuther, C. G. Dotti, and K. Simons.** 1998. Cholesterol depletion inhibits the generation of beta-amyloid in hippocampal neurons. Proc. Natl. Acad. Sci. USA **95:**6460–6464.
66a. **Sirena, D., B. Lilienfeld, M. Eisenhut, S. Kaelin, K. Boucke, R. R. Beeli, L. Vogt, C. Ruedl, M. F. Bachmann, U. F. Greber, and S. Hemmi.** The human membrane cofactor CD46 is a receptor for the species B adenovirus serotype 3. J. Virol., in press.
67. **Snyers, L., H. Zwickl, and D. Blaas.** 2003. Human rhinovirus type 2 is internalized by clathrin-mediated endocytosis. J. Virol. **77:**5360–5369.
68. **Steer, C. J., M. Bisher, R. Blumenthal, and A. C. Steven.** 1984. Detection of membrane cholesterol by filipin in isolated rat liver coated vesicles is dependent upon removal of the clathrin coat. J. Cell Biol. **99:**315–319.
69. **Subtil, A., I. Gaidarov, K. Kobylarz, M. A. Lampson, J. H. Keen, and T. E. McGraw.** 1999. Acute cholesterol depletion inhibits clathrin-coated pit budding. Proc. Natl. Acad. Sci. USA **96:**6775–6780.
70. **Suomalainen, M., M. Y. Nakano, K. Boucke, S. Keller, and U. F. Greber.** 2001. Adenovirus-activated PKA and p38/MAPK pathways boost microtubule-mediated nuclear targeting of virus. EMBO J. **20:**1310–1319.
71. **Superti, F., L. Seganti, F. M. Ruggeri, A. Tinari, G. Donelli, and N. Orsi.** 1987. Entry pathway of vesicular stomatitis virus into different host cells. J. Gen. Virol. **68:**387–399.
72. **Tobert, J. A.** 2003. Lovastatin and beyond: the history of the HMG-CoA reductase inhibitors. Nat. Rev. Drug Discov. **2:**517–526.
73. **Trotman, L. C., N. Mosberger, M. Fornerod, R. P. Stidwill, and U. F. Greber.** 2001. Import of adenovirus DNA involves the nuclear pore complex receptor CAN/Nup214 and histone H1. Nat. Cell Biol. **3:**1092–1100.
74. **van Deurs, B., K. Roepstorff, A. M. Hommelgaard, and K. Sandvig.** 2003. Caveolae: anchored, multifunctional platforms in the lipid ocean. Trends Cell Biol. **13:**92–100.
75. **Varga, M. J., C. Weibull, and E. Everitt.** 1991. Infectious entry pathway of adenovirus type 2. J. Virol. **65:**6061–6070.
76. **Wang, K. N., S. Huang, A. Kapoormunshi, and G. Nemerow.** 1998. Adenovirus internalization and infection require dynamin. J. Virol. **72:**3455–3458.
77. **Watarai, M., S. Makino, Y. Fujii, K. Okamoto, and T. Shirahata.** 2002. Modulation of Brucella-induced macropinocytosis by lipid rafts mediates intracellular replication. Cell Microbiol. **4:**341–355.
78. **Weber, J.** 1976. Genetic analysis of adenovirus type 2. III. Temperature sensitivity of processing of viral proteins. J. Virol. **17:**462–471.